

Thermodynamic Properties of Correlated Strongly Degenerate Plasmas

V.S. Filinov, P.R. Levashov, V.E. Fortov

*Russian Academy of Sciences, High Energy Density Research Center
Izhorskaya street 13-19, Moscow 127412, Russia*

M. Bonitz

*Universität Rostock, Fachbereich Physik
Universitätsplatz 3, 18051 Rostock, FRG
E-mail: micha@elde.mpg.uni-rostock.de*

An efficient numerical approach to equilibrium properties of strongly coupled systems which include a subsystem of fermionic quantum particles and a subsystem of classical particles is presented. It uses an improved path integral representation of the many-particle density operator and allows to describe situations of *strong coupling and strong degeneracy*, where analytical theories fail. A novel numerical method is developed, which allows to treat degenerate systems with full account of the spin statistics. Numerical results for thermodynamic properties such as internal energy, pressure and pair correlation functions are presented over a wide range of degeneracy parameter.

1 Introduction

Thermodynamic properties of correlated Fermi systems continue to attract the interest of researches in many fields, including plasmas, condensed matter and astrophysics. All present theories have practical difficulties. Quantum kinetic methods, including the Kadanoff-Baym equations^{1,2}, easily handle quantum and spin effects, but they become extremely complicated when correlation effects can not be treated perturbatively. It is, therefore, important to consider alternative approaches, such as Monte Carlo simulations^{3,4}, as they allow for an efficient treatment of strong coupling phenomena. However, they still have difficulties in incorporating quantum and spin statistics effect. In particular, there has been remarkable progress in applying path integral quantum Monte Carlo (PIMC) techniques to Bose systems⁵ and Coulomb systems, see e.g. ^{4,7} and Ref. ⁸ for an overview. Nevertheless, there has still been one major obstacle preventing efficient modelling of Fermi systems – the so-called sign problem resulting from summation over all permutations of the density matrix. In this paper, we present a different path integral representation in which no sign problem appears.

2 Path-Integral Monte Carlo Methods

As is well known the thermodynamic properties of a quantum system of N particles are fully determined by the partition function Z and, consequently, by the density matrix

$$Z = \int_V dq \rho(q, 0; q, \beta), \quad \rho(q, 0; q', \beta) = \langle q | \hat{\rho} | q' \rangle, \quad (1)$$

where $\hat{\rho} = \exp\{-\beta\hat{H}\}$, $\beta = 1/kT$, and q comprises the coordinates of all particles, $q \equiv \{\mathbf{q}_1, \mathbf{q}_2, \dots, \mathbf{q}_N\}$. With an analytical expression for the density matrix given, one can use e.g. Monte Carlo methods^{3,4} to evaluate the partition function and thermodynamic quantities. However, for a quantum system, ρ is, in general, not known, but can be constructed from its known high-temperature limit by means of a decomposition into $n+1$ factors, each of which corresponds to the density matrix at an $n+1$ times higher temperature^{6,3,4,8,9},

$$\rho(q, 0; q', \beta) = \int_V dq^{(1)} \dots dq^{(n)} \rho(q, 0; q^{(1)}, \tau^{(1)}) \times \dots \times \rho(q^{(n)}, \tau^{(n)}; q', \beta), \quad (2)$$

where $\tau^{(i+1)} - \tau^{(i)} = \Delta\beta = \beta/(n+1)$. Eq. (2) lets one view the N -particle state as a loop consisting of $n+1$ vertices (“beads”) located at intermediate coordinates $q^{(i)}$ which is closed, i.e. $q^{(n+1)} \equiv q^{(1)}$, due to the trace in Eq. (1). For quantum systems of bosons (fermions), furthermore, the spin statistics has to be taken into account requiring to perform an (anti-)symmetrization of the density matrix, after which Eq. (2) obtains the form (for simplicity, the spin variables are not written explicitly)

$$\rho(q, 0; q', \beta) = \frac{1}{N!} \sum_P (\pm 1)^{\kappa_P} \int_V dq^{(1)} \dots dq^{(n)} \rho(q, 0; q^{(1)}, \tau^{(1)}) \times \dots \times \rho(q^{(n)}, \tau^{(n)}; Pq', \beta), \quad (3)$$

where P denotes an arbitrary N -particle permutation of the particle coordinates, and κ_P is its parity.

The unknown density matrix (3) is efficiently computed by approximating the ρ 's on the r.h.s. of Eq. (3) by the high-temperature density matrix ρ^{hT} . For potentials which are bounded from below the simplest choice is^{3,4,8,9}

$$\begin{aligned} \rho^{hT}(q, \tau; q', \tau') &= \rho_0(q, \tau; q', \tau') e^{-(\tau' - \tau)U(q)}, \\ \rho_0(q, \tau; q', \tau') &= \frac{1}{\lambda_{\Delta}^{3N}} e^{-\pi|q - q'|^2 / \lambda_{\Delta}^2}, \end{aligned} \quad (4)$$

where ρ_0 is the free-particle density matrix, U is the potential energy, and λ_Δ is the thermal DeBroglie wave length corresponding to the higher temperature $kT' = 1/\Delta\beta$, $\lambda_\Delta^2 \equiv 2\pi\hbar^2(\tau - \tau')/m$. It is well known that for $n \rightarrow \infty$, ρ^{hT} converges to the exact density matrix ρ . Notice that the factorization of ρ^{hT} into a kinetic and potential energy term, Eq. (4), is an approximation also. The error made thereby is of the order of the variation of U on the spatial scale λ_Δ and thus vanishes with $n \rightarrow \infty$. This holds also for an repulsive Coulomb potential, whereas the attractive electron-ion interaction has to be represented by a bounded from below effective pair potential^{2,3,10}.

3 Thermodynamic quantities of dense quantum plasmas

The sign problem is solved by a simple transform of the intermediate electron coordinates¹¹. To this end, we rewrite the partition function (1), now explicitly including the (classical) ion component, $N_e = N_i = N$,

$$Z(N, V, \beta) = \frac{Q(N_e, N_i, \beta)}{N_e! N_i! \lambda_i^{3N_i} \lambda_\Delta^{3N_e}},$$

with
$$Q(N_e, N_i, \beta) = \int_V dq dr d\xi \rho(q, [r], \beta). \quad (5)$$

Here, the notation q is retained for the ions. $[r]$ summarizes the electron coordinates with r denoting the coordinates at the beginning of the loop and $\xi^{(1)}, \dots, \xi^{(n)}$ the dimensionless distances between neighboring vertices. Thus, explicitly, $[r] = [r, r + \lambda_\Delta \xi^{(1)}, r + \lambda_\Delta(\xi^{(1)} + \xi^{(2)}), \dots]$, and $q, r, \xi^{(i)}$ each are $3N$ -dimensional vectors. For the density matrix in Eq. (5) we have^{3,10}

$$\rho(q, [r], \beta) = \sum_{s=0}^N \rho_s(q, [r], \beta) = \sum_{s=0}^N \frac{C_N^s}{2^N} e^{-\beta U(q, [r], \beta)} \prod_{l=1}^n \prod_{p=1}^N \phi_{pp}^l \det |\phi_{ab}^{n,1}|_s,$$

where
$$U(q, [r], \beta) = U^i(q) + \frac{1}{n+1} \sum_{l=0}^n \{U_l^e([r], \beta) + U_l^{ei}(q, [r], \beta)\}, \quad (6)$$

and U^i denotes the ion-ion interaction energy, whereas U_l^e denotes the interaction energy corresponding to the electronic vertex “l”, and U_l^{ei} means the analogous electron-ion contribution. Furthermore, $\phi_{pp}^l \equiv \exp[-\pi|\xi_p^l|^2]$ arises from the kinetic energy density matrix ρ_0 , while ϕ_{ab} is the exchange matrix the elements of which are given by $\phi_{ab}^{n,1} \equiv \exp[-\pi|(r_a - r_b)/\lambda_\Delta + \sum_{k=1}^n \xi_a^k|^2]$. The determinant arises from the sum over the permutations, cf. Eq. (3). Finally, s is the number of electrons having the same spin projection. Due to the spin

variables, the exchange matrix contains two zero submatrices which are related to electrons with opposite spin projection.

As an example of applying our method to thermodynamic properties, we provide the result for the equation of state, $\beta p = \partial \ln Q / \partial V = [\alpha \partial \ln Q / 3V \partial \alpha]_{\alpha=1}$,

$$\begin{aligned} \frac{\beta p V}{2N} = & 1 + \frac{1}{6NQ} \sum_{s=0}^N \int dq dr d\xi \rho_s(q, [r], \beta) \left\{ \sum_{p<t}^{N_i} \frac{\beta e^2}{|q_{pt}|} + \sum_{p<t}^{N_e} \frac{\beta e^2}{(n+1)|r_{pt}|} \right. \\ & - \sum_{p=1}^{N_i} \sum_{t=1}^{N_e} \frac{|x_{pt}|}{n+1} \frac{\partial \beta \Phi^{ie}}{\partial |x_{pt}|} + \sum_{p=1}^n \sum_{p<t}^{N_e} \frac{\beta e^2 \langle r_{pt}^l | r_{pt} \rangle}{(n+1)|r_{pt}^l|^3} \\ & \left. - \sum_{l=1}^n \sum_{p=1}^{N_i} \sum_{t=1}^{N_e} \frac{\langle x_{pt}^l | x_{pt} \rangle}{(n+1)|x_{pt}^l|} \frac{\partial \beta \Phi^{ie}}{\partial |x_{pt}^l|} + \frac{\alpha}{\det|\phi_{pt}^{n,1}|_s} \frac{\partial \det|\phi_{pt}^{n,1}|_s}{\partial \alpha} \right\}. \quad (7) \end{aligned}$$

Here, Φ^{ie} is the effective electron-ion pair potential, α is a scaling parameter, $\langle \dots | \dots \rangle$ denotes the scalar product, and q_{pt}, ξ_{pt}, r_{pt} and x_{pt} are differences of two coordinate vectors: $q_{pt} \equiv q_p - q_t$, $r_{pt} \equiv r_p - r_t$, $\xi_{pt}^k \equiv \xi_p^k - \xi_t^k$, $r_{pt}^l \equiv r_p^l - r_t^l + \lambda_\Delta \sum_{k=1}^l \xi_{pt}^k$, and $x_{pt}^l \equiv r_p^l - q_t + \lambda_\Delta \sum_{k=1}^l \xi_p^k$. We underline that introducing the dimensionless coordinate components ξ removes a substantial part of the complicated temperature and volume dependence from the density

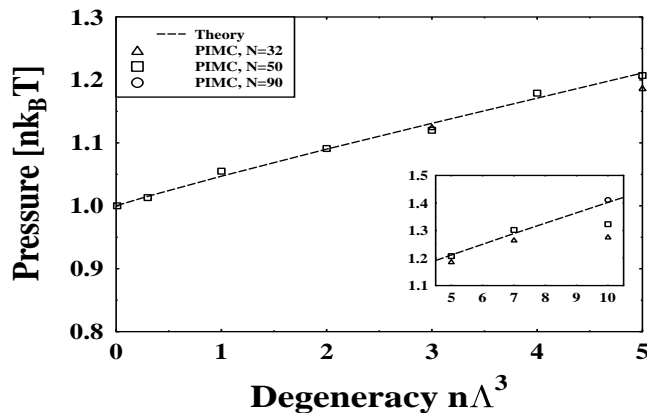


Figure 1: Pressure of a mixture of ideal electrons and protons. Spin statistics of the electrons is fully included, protons are treated classically.

matrix (6). This turns out to be crucial in the computation of thermodynamic quantities as they involve derivatives of the partition function with respect to V or β . Furthermore, the anti-symmetrization problem is reduced to computing the determinant of ϕ_{pt} , and no explicit summation over permutations with

alternating sign is required. In fact, for each fixed particle configuration, the absolute value of each sum in curly brackets in Eq. (7) is bounded as $n \rightarrow \infty$, which is sufficient to eliminate the sign problem completely. This enables us to evaluate thermodynamic properties of quantum plasmas without further approximations on the density matrix and the integration region. For the numerical calculations, we use the standard Metropolis Monte Carlo procedure in which the probability of sampling configurations is proportional to $|\rho_s|$, while the sign of ρ_s is included into the weight function of the particle configuration. Expressions similar to (7) are readily derived for other thermodynamic quantities and, along with more details, will be given elsewhere.

4 Numerical results

Using the above results, we have performed a series of calculations for a two-component electron-proton plasma. Notice that this first-principle treatment of the elementary plasma particles (physical picture) does fully include bound states. Of course, the quality of describing their properties depends on the potential Φ^{ie} for which we chose an effective quantum pair potential originally derived by Kelbg which is the exact high-temperature limit, e.g. ². Thus, by increasing the number of electronic vertices n , in principle, any desired accuracy can be achieved. To test the quality of the reproduction of quantum and spin statistics effects, we first consider a mixture of ideal electrons and protons for which the thermodynamic quantities are known analytically, e.g. ².

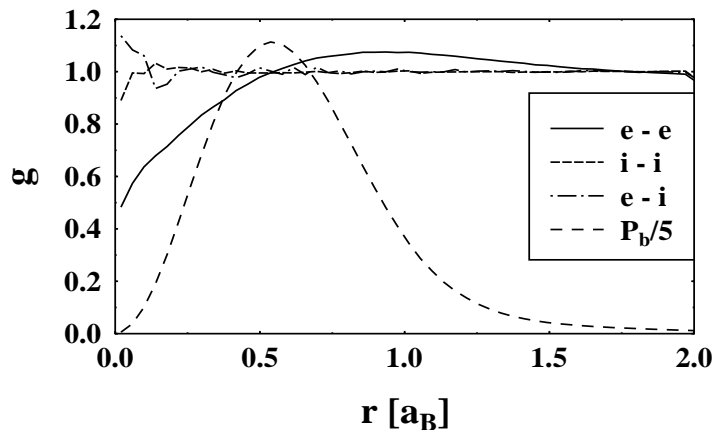


Figure 2: Pair correlation functions for non-interacting electrons and protons at $n\Lambda^3 = 4$. The decrease of g_{ee} for small distances reflects the Pauli principle. Also shown is the vertex separation distribution P_b .

Fig. 1 shows our numerical results for the pressure together with the theoretical curve. The agreement, up to values of the degeneracy parameter $\chi \equiv n\lambda^3$ as large as 5 is remarkable. Even with only $N = 16$ electrons and protons deviations are rather small. One clearly sees that increasing the number of particles improves the numerical results systematically.

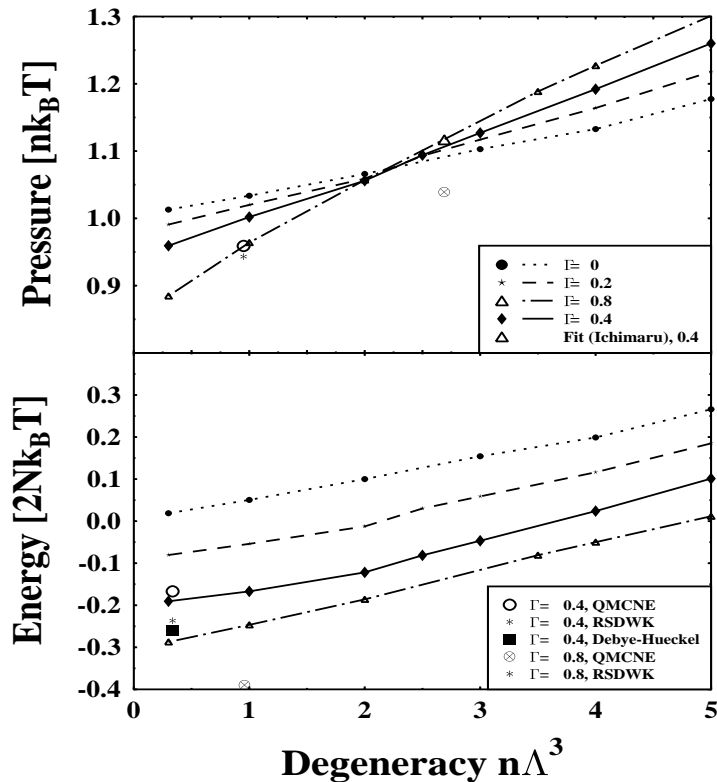


Figure 3: Pressure (upper figure) and total energy $-3NkT$ (lower figure) of an electron-proton plasma for different values of the classical coupling parameter Γ . For comparison, results of other groups are shown: QMCNE - quantum MC without exchange, RSDWK - analytical model of Rieman et al. ¹².

Fig. 2 shows the correspondig e-e, i-i and e-i pair correlation functions. As expected, the functions g_{ei} and g_{ii} are identical to one. The fluctuations at small distances reflect the maximal statistical error of the MC simulation and rapidly decay with increasing distance. The decay at large distances is a consequence of the periodic boundary conditions in the MC simulation. In contrast, the electron-electron correlation function decays at small distances reaching

0.5 at $r = 0$ which is the expected result for particles with spin 1/2. Notice further the maximum of g_{ee} which appears around the thermal wavelength λ_e and reflects weak ordering due to Fermi repulsion. To characterize the strength of quantum effects, we also show the probability distribution of distances between neighboring vertices on the electron loops P_b . It has a maximum on a distance of the order of $\lambda_\Delta/\sqrt{\pi}$.

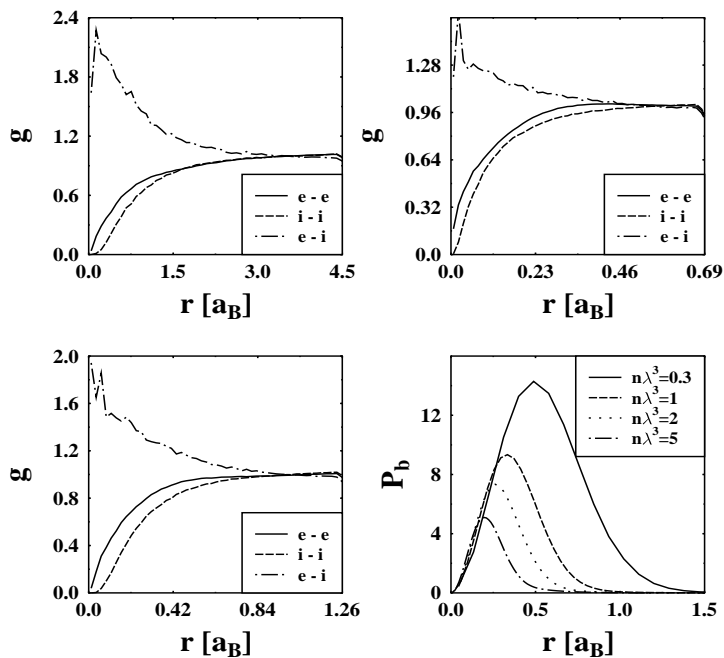


Figure 4: Pair correlation functions for a correlated electron-proton plasma with $\Gamma = 0.4$ and different values of the degeneracy parameter. Notice the different length scales. Bottom right figure shows the vertex separation distribution P_b (arbitrary units, see text).

Let us now turn to the case of interacting electrons and protons. We have performed a series of calculations in which the classical coupling parameter $\Gamma = (4\pi n_e/3)^{1/3} e^2/4\pi\epsilon_0 kT$ was kept constant while the degeneracy was varied. The results for the pressure and energy are presented in Fig. 3. One can see that for weak coupling and small degeneracy parameters, $\chi < 0.5$, exchange effects are small, and QMC simulations without exchange (open circles) are close to our results. However, with increasing χ and Γ , the deviations are growing rapidly. Even stronger are the discrepancies with analytical theories which are constructed as perturbations expansions, and thus are limited to small values

of χ and Γ . Most strikingly is the decrease of the energy as a function of χ predicted by the analytical models and QMC without exchange, which is in contrast to our results which show an increase for all values of Γ . Finally, Fig. 4 shows the pair correlation functions for intermediate coupling, $\Gamma = 0.4$ for various degrees of degeneracy. Now, due to Coulomb repulsion, at small distances g_{ee} and g_{ii} decay to zero. However, the decay of g_{ee} is essentially different from that of the proton-proton function, despite the identical Coulomb force. The reason are quantum exchange and tunneling effects in the electron subsystem which compete with the Coulomb repulsion.

Acknowledgments

We acknowledge support from the Deutsche Forschungsgemeinschaft (Mercator-Programm) for VSF and stimulating discussions with B. Bernu, D. Ceperley, D. Kremp and M. Schlanges.

References

1. L.P. Kadanoff and G. Baym, *Quantum Statistical Mechanics*, Addison-Wesley Publ. Co. Inc., 2nd ed., 1989.
2. W.D. Kraeft, D. Kremp, W. Ebeling, and G. Röpke, *Quantum Statistics of Charged Particle Systems*, Akademie-Verlag Berlin 1986
3. V.M. Zamalin, G.E.Norman, and V.S. Filinov, *The Monte Carlo Method in Statistical Thermodynamics*, Nauka, Moscow 1977 (in Russian).
4. *The Monte Carlo and Molecular Dynamics of Condensed Matter Systems*, K. Binder and G. Cicotti (eds.), SIF, Bologna 1996
5. D. M. Ceperley, Rev. Mod. Phys. **65**, 279 (1995)
6. R.P. Feynman, and A.R. Hibbs, *Quantum mechanics and path integrals*, McGraw-Hill, New York 1965
7. C. Pierleoni, B. Bernu, D.M. Ceperley, and W.R. Magro, Phys. Rev. Lett. **73**, 2145 (1994)
8. D.M. Ceperley, in Ref. ⁴, pp. 447-482
9. *Classical and Quantum Dynamics of Condensed Phase Simulation*, B.J.Berne, G.Ciccotti and D.F.Coker eds., World Scientific, Singapore 1998
10. V.S. Filinov, High Temp. **13**, 1065 (1975) and **14**, 225 (1976)
11. V.S. Filinov, and M. Bonitz, subm. to Phys. Rev. Lett.
12. J. Riemann, M. Schlanges, H.E. DeWitt, and W.D. Kraeft, Proceedings of the International Conference on Strongly Coupled Plasmas, W.D. Kraeft and M. Schlanges (eds.), World Scientific, Singapore 1996, p. 82